Numerical simulation of two-phase immiscible incompressible flows in heterogeneous porous media with capillary barriers

Igor Mozolevski, Luciane Schuh

Numerical simulation of two-phase immiscible incompressible flows in heterogeneous porous media with capillary barriers

I.Mozolevski[a,1], L. Schuh[a,1]

[a]*Departamento de Matemática, Universidade Federal de Santa Catarina, 88040-900, Florianópolis-SC, Brasil*

Abstract

We present a new version of the sequential discontinuous Galerkin method introduced in [25] for two-phase immiscible incompressible flows in heterogeneous porous media with a discontinuous capillary field. Here, a new implementation of the extended interface condition, that does not use the threshold saturation value at the interface and permits treatment of different residual saturations in different rocks, is considered. Another novel ingredient is the implicit treatment of the diffusion term and the non-linear interface conditions in the saturation equation. The proposed method is validated in two-dimensional test cases and confirms theoretically known optimal orders of convergence. The numerical experiments demonstrate that for two-dimensional interface problems the method exhibits better performance on moderately refined meshes, which is particularly important for multidimensional heterogeneous problems related to realistic field studies. We consider also two heterogeneous five-spot benchmark problems to assess the potential of the proposed method in simulations of reservoirs with discontinuous permeability and capillary pressure fields in different types of rock.

Keywords:
discontinuous Galerkin, two-phase flows, heterogeneous porous media, discontinuous capillary pressure, interface condition, weighted averages, secondary oil recovery
PACS: 02.70.Dh, 47.56.+r, 02.60.Cb
2000 MSC: 65M60, 65N30, 76T99, 76S05

1. Introduction

Numerical simulation of two-phase immiscible incompressible flows through heterogeneous porous media is significantly complicated by the discontinuity of capillary pressure fields at interfaces that separate subdomains with different rock properties. In such a case, the saturation is forced to be discontinuous at the interface to guarantee the capillary pressure continuity if both phases are present on both sides of the interface; when one of the

Email addresses: Igor.Mozolevski@mtm.ufsc.br (I.Mozolevski), luciane@mtm.ufsc.br (L. Schuh)
[1]Partially supported by CNPq, Brazil

phases is absent, the capillary pressure can be discontinuous also owing to the difference between the entry pressures of the different rocks. For such applications, the global pressure and the saturation can exhibit strong discontinuities due to drastic (up to some orders) permeability changes and swift variations in the capillary forces. The development of numerical methods for two-phase flows in heterogeneous porous media, which besides being compatible with the non-linearity and degeneracy of the pressure and the saturation equations, should satisfactorily deal with this discontinuity of the saturation and the global pressure is a relevant and challenging problem.

The system of equations governing two-phase immiscible incompressible flows in porous media, is usually considered in global pressure - fractional flow formulation, see e.g. [5, 14, 16, 33]. In such formulation the system consists of a nonlinear elliptic Darcy-type equation for the global pressure and a nonlinear parabolic equation with degenerate diffusion term for the saturation, which are coupled by means of the total velocity, recuperated from Darcy's equation. In heterogeneous porous media, capillary force discontinuities require nonlinear interface conditions for the global pressure and the saturation, owing to which both variables can exhibit a nonzero jump at the interface, see [43, 28, 6, 21] for a detailed discussion.

During recent decades mathematical analysis and numerical simulation of two-phase flows in heterogeneous porous media have been the subject of investigation of many researchers and practitioners owing to important applications in petroleum engineering and hydrology. The well-posedness of the interface problem with nonlinear interface conditions was analyzed in [7, 2, 6, 21, 10, 12, 11, 13]. A semi-analytical similarity solution for the saturation equation in a pure diffusion case and homogeneous media was presented in [38], [17], [39]. For heterogeneous media similarity solution to the interface problem for saturation equation in diffusion case was obtained in [44]. Later the solution was extended in [30] to the saturation equation in homogeneous medium, that includes advective term corresponding to more general entry fluxes, and to the case of a medium with a simple heterogeneity in [31].

Many numerical schemes have been developed for two-phase flows in heterogeneous media with discontinuous capillary forces. Finite volume schemes have been proposed in [28, 21, 11, 8] and a convergence of the numerical solution to a weak solution to the problem was demonstrated. A combination of a mixed finite elements method for the pressure equation and discontinuous Galerkin (dG) for saturation equation was suggested in [40], [35].

Recently, discontinuous Galerkin methods have been effectively used for developing numerical schemes for the sequential global pressure-fractional flow formulation of two-phase flows in porous media. Local conservation properties, the potential to capture fronts sharply and flexibility in the use of non-matching meshes in regions of different rock type are, probably, some of the most attractive features offered by dG methods for these kinds of problems. A mathematical analysis of dG methods and implementation techniques encompassing various partial differential equations can be found in recent monographs [19, 42, 34].

Different versions of dG methods have been considered for mathematical models of flow in homogeneous and heterogeneous media, but these do not include the discontinuity of capillary forces, see e.g. [4], [3], [36], [29], [22]. Firstly, a sequential dG method for two phase flows in heterogeneous porous media that includes capillary barriers at interfaces was introduced in [25]. The method uses symmetric interior penalties dG for both pressure and

saturation equations, in which, exploring the advantages of dG methods, the nonlinear interface conditions are implemented weakly through adequate design of the symmetrization term and penalties on interelement jumps at the interface. An effective algorithm of reconstruction in the Raviart–Thomas(–Nédélec) finite element spaces of the conservative total velocity from the discontinuous potential, suggested in [26, 24], was extended to the interface problem. The diffusivity-dependent weighted averages technique [27] was used to cope with degeneracy in the saturation equation and with global pressure and saturation discontinuity owing heterogeneity of the media. This paper is devoted to the further development and two-dimensional validation of the dG method, introduced in [25]. In particular, we study two phase incompressible immiscible flows in two-dimensional domains with heterogeneous sub-domains of complex geometry. In such a case the trapping effect can take a more complicated form owing to different mobility of the fluid and different permeability of the rock in different regions in combination with the presence of capillary barriers at interfaces.

The paper is organized as follows. In section 2 we present a short description of the mathematical model of two-phase flow in heterogeneous porous media in the global pressure - fractional flow formulation, introduce basic assumptions regarding the coefficients of the equations and discuss the respective interface conditions. The formulation of the sequential dG method for the considered interface problem is presented in section 3. Here we introduced a new implementation of the nonlinear interface condition and redesign the dG sequential scheme for the saturation equation, considering implicit treatment of the elliptic part of the saturation equation and the non-linear interface condition. The efficiency and the accuracy of the method are validated in section 4. Firstly, we analyze numerically for the two - dimensional case the order of convergence of the weighted average symmetric dG for the non-linear advection-diffusion equation (test case 1) and the order of convergence of the sequential dG for a coupled system of equations (test case 2). Then, in test case 3, we study the convergence of the numerical solution of implicit and explicit versions of the dG method to a semi analytical solution of the interface problem for the degenerate diffusion equation. Finally, in section 4, using the sequential dG method introduced, we consider the numerical simulation of two phase flow in the heterogeneous five-spot problem with different rock properties in order to demonstrate the potential of the method in realistic field studies in two-dimensional heterogeneous problems with capillary barriers.

2. Problem formulation

Let Ω be a bounded, open, polyhedral domain in $\mathbb{R}^d$, $d = 2, 3$ with boundary $\partial\Omega$. Let us suppose that the interior of Ω is a porous medium that can admit different physical characteristics in different sub-domains; for simplicity we shall limit this study to considering two subdomain only. So let us suppose that Ω is divided into two open, polyhedral subdomains $\Omega^{(\beta)}, \beta = 1, 2$ such that $\overline{\Omega} = \overline{\Omega^{(1)}} \cup \overline{\Omega^{(2)}}$ and $\Omega^{(1)} \cap \Omega^{(2)} = \emptyset$ and let $\Gamma := \partial\Omega^{(1)} \cap \partial\Omega^{(2)}$ denote the interface. Let us denote the outward normal to $\partial\Omega$ by η and the normal to Γ, oriented outward to $\Omega^{(1)}$, by η_Γ. In what follows, for any real function (distribution) u, defined in Ω, we will denote its restriction to $\Omega^{(\beta)}$ by $u^{(\beta)}$.

Thus, let us consider a two-phase immiscible incompressible flow in Ω where the wetting

and the non-wetting phases are characterized by their saturation s_α and phase pressure p_α; here and in the sequel we use index $\alpha = w$ for the wetting and $\alpha = n$ for the non-wetting phase. From the saturation and pressure laws we have

$$s_w + s_n = 1, \tag{1}$$
$$p_n - p_w = \pi(s_n), \tag{2}$$

where π is the capillary pressure.

Let us suppose that the porous medium in each subdomain $\Omega^{(\beta)}, \beta = 1, 2$ has different porosity $\Phi^{(\beta)}$ and intrinsic (absolute) permeability $K^{(\beta)}$ and that (for simplicity) both quantities are constant in each subdomain. In what follows we will designate by $s = s_n$ the non-wetting phase saturation omitting also the index β when it is clear in which subdomain the saturation is considered. We denote by $s_{\alpha r}^{(\beta)}$ the residual saturation of the phase α is the subdomain $\Omega^{(\beta)}$ and denote by $s_{ne}^{(\beta)}(s) = (s - s_{nr}^{(\beta)})/(1 - s_{nr}^{(\beta)} - s_{wr}^{(\beta)}), \quad s_{ne}^{(\beta)} : [s_{nr}^{(\beta)}, 1 - s_{wr}^{(\beta)}] \to [0, 1]$ the effective saturation of the non-wetting phase.

According to the Leverett model the capillary pressure (cf. [37])

$$\pi^{(\beta)}(s) = \sigma \sqrt{\frac{\Phi^{(\beta)}}{K^{(\beta)}}} J^{(\beta)}(s_{ne}^{(\beta)}(s)), \tag{3}$$

where σ is the interfacial tension and $J^{(\beta)} : [0, 1) \to \mathbb{R}$ is the Leverett function. The value $P_e^{(\beta)} = \sigma \sqrt{\frac{\Phi^{(\beta)}}{K^{(\beta)}}} J^{(\beta)}(0)$ is known as the entry pressure; this is the minimum pressure that is needed for a non-wetting phase to enter a medium that is saturated by the wetting phase. The entry pressure is particularly important for flows in heterogeneous porous media: if the entry pressures are different on the different sides of the interface then, as is well known, cf. [43, 21], the capillary pressure can be discontinuous across the interface and the extended pressure condition is needed. In such a situation the saturation equation can admit solutions describing the entrapment of the non-wetting phase in one of the subdomains, see e.g [43, 44].

Let us denote by $kr_\alpha^{(\beta)}(s) = \widehat{kr}_\alpha^{(\beta)}(s_{ne}^{(\beta)}(s))$ the relative permeability of the phase α in $\Omega^{(\beta)}$.

Assumption 1. *In the sequel we will suppose that the following assumptions are valid for* $\beta = 1, 2$*:*

1. *function* $J^{(\beta)} \in C^1[0, 1) \cap L^1(0, 1)$ *is strictly increasing with* $J^{(\beta)}(0) > 0$, $J^{(1)}(s) \neq J^{(2)}(s) \quad \forall s \in [0, 1)$ *and* $\lim_{s \to 1^-} J^{(\beta)}(s) = +\infty$*;*
2. *function* $\widehat{kr}_w^{(\beta)} \in C^1[0, 1]$ *is strictly decreasing with* $\widehat{kr}_w^{(\beta)}(0) = 1$ *and* $\widehat{kr}_w^{(\beta)}(1) = 0$*;*
3. *function* $\widehat{kr}_n^{(\beta)} \in C^1[0, 1]$ *is strictly increasing with* $\widehat{kr}_n^{(\beta)}(0) = 0$ *and* $\widehat{kr}_n^{(\beta)}(1) = 1$.

Let us consider the governing equations of two-phase immiscible incompressible flows through the heterogeneous porous medium Ω in the classical [14] global pressure/fractional flow formulation:

for a given simulation time T, find (p, s) that satisfies in $\Omega^{(\beta)} \times [0, T]$ for each $\beta = 1, 2$ the following system of partial differential equations

$$\begin{aligned} &- \nabla \cdot \left(\kappa^{(\beta)}(s)\nabla p\right) = F_w^{(\beta)} + F_n^{(\beta)}, \\ &\mathbf{q}^{(\beta)} = -\kappa^{(\beta)}(s)\nabla p, \\ &\Phi^{(\beta)}\partial_t s + \nabla \cdot \left(-\epsilon^{(\beta)}(s)\nabla s + \mathbf{q}^{(\beta)} f_n^{(\beta)}(s)\right) = F_n^{(\beta)}, \end{aligned} \tag{4}$$

where $\lambda_\alpha^{(\beta)} = kr_\alpha^{(\beta)}/\mu_\alpha$ denotes the mobility of the phase α, μ_α is the viscosity of the fluid, $\lambda^{(\beta)} = \lambda_w^{(\beta)} + \lambda_n^{(\beta)}$ denotes the total mobility, $f_\alpha^{(\beta)} = \lambda_\alpha^{(\beta)}/\lambda^{(\beta)}$ denotes the fractional flux of the phase α, $\kappa^{(\beta)} = \lambda^{(\beta)} K^{(\beta)}$, $\epsilon^{(\beta)} = \lambda_w^{(\beta)} f_n^{(\beta)} K^{(\beta)} (\pi^{(\beta)})'$, and $F_\alpha^{(\beta)}$ denotes volumetric sources or sinks of phase α in medium β. We will suppose that the diffusion coefficient in the saturation equation and the fractional flux have the following property.

Assumption 2. *Function*

$$\epsilon^{(\beta)} = \frac{kr_w^{(\beta)} kr_n^{(\beta)} (\pi^{(\beta)})'}{\mu_n kr_w^{(\beta)} + \mu_w kr_n^{(\beta)}} K^{(\beta)}$$

is Lipschitz continuous and the fractional flux $f_n^{(\beta)}$ is increasing function on $[s_{nr}^{(\beta)}, 1 - s_{wr}^{(\beta)}]$, $\beta = 1, 2$.

The unknowns in this system are the non-wetting phase saturation s and the global pressure, which is defined in terms of wetting or non-wetting phase pressure (see e.g [14]) as

$$p^{(\beta)} = p_w^{(\beta)} + \pi^{(\beta)}(s_{nr}^{(\beta)}) + \int_{s_{nr}^{(\beta)}}^{s} f_n^{(\beta)} (\pi^{(\beta)})' = p_n^{(\beta)} - \int_{s_{nr}^{(\beta)}}^{s} f_w^{(\beta)} (\pi^{(\beta)})'. \tag{5}$$

At the interface we impose the extended interface conditions (see e.g. [14, 43, 21] and [25]) using different but equivalent formulation. Let us suppose, to fix ideas, that $P_e^{(1)} < P_e^{(2)}$ and

$$\pi^{(1)}(s) < \pi^{(2)}(s) \quad \forall s \in \bigcap_{\beta=1,2} [s_{nr}^{(\beta)}, 1 - s_{wr}^{(\beta)}).$$

Let us denote by $\overline{\pi}^{(\beta)} : \mathbb{R} \to [s_{nr}^{(\beta)}, 1 - s_{wr}^{(\beta)})$ the extension to $\mathbb{R}$ of the inverse function for $\pi^{(\beta)}$

$$\bar{\pi}^{(\beta)}(p) = \begin{cases} s_{nr}^{(\beta)}, & \text{if } p < P_e^{(\beta)}, \\ (\pi^{(\beta)})^{-1}(p), & \text{if } p \geq P_e^{(\beta)}, \end{cases} \tag{6}$$

and let us introduce the jump of saturation at the interface by

$$j_s(\xi) = \xi - \bar{\pi}^{(2)}(\pi^{(1)}(\xi)), \text{ if } \xi \in [s_{nr}^{(1)}, 1 - s_{wr}^{(1)}). \tag{7}$$

Note that j_s is a continuous function in $[s_{nr}^{(1)}, 1 - s_{wr}^{(1)})$ and owing to the definition of the extended inverse function $\bar{\pi}^{(\beta)}$ permits to define jump for different values of the residual phase saturations $s_{\alpha r}^{(\beta)}$ in each subdomain avoiding the necessity of the rescaling, se e.g. [25].

Differently from the definitions in cited previous publications, this definition not depends explicitly on the threshold saturation $s^* \in (s_{nr}^{(1)}, 1 - s_{wr}^{(1)})$ such that

$$\pi^{(1)}(s^*) = \pi^{(2)}(s_{nr}^{(2)}),$$

that exists and is unique owing to the item 1 of the Assumption 1. Nevertheless it is easy to see that

$$j_s(\xi) = \begin{cases} \xi - s_{nr}^{(2)}, & \text{if } s_{nr}^{(1)} \le \xi \le s^*, \\ (\pi^{(2)})^{-1}(\pi^{(1)}(\xi)), & \text{if } s^* < \xi \le 1 - s_{wr}^{(1)}; \end{cases} \tag{8}$$

so this definition of the jump of the saturation exactly coincides with the one from [25], and, consequently, with the extended interface conditions for the saturation at the interface.

Let $\mathbf{r}^{(\beta)}(p, \xi; s) = -\epsilon^{(\beta)}(s)\nabla s + \mathbf{q}^{(\beta)}(p, \xi) f_n^{(\beta)}(s)$ be the volumetric flux of the saturation. The interface conditions for saturation impose the continuity of the normal component of $\mathbf{r}$ at the interface (due to the mass conservation) and prescribe the jump of the saturation at the interface to satisfy the extended pressure condition (c.f. [21, 25]):

$$\begin{cases} \mathbf{r}^{(1)}(p^{(1)}, s^{(1)}; s^{(1)}) \cdot \eta_\Gamma = \mathbf{r}^{(2)}(p^{(2)}, s^{(2)}; s^{(2)}) \cdot \eta_\Gamma \quad \text{at } \Gamma \\ s^{(1)} - s^{(2)} = j_s(s^{(1)}) \quad \text{at } \Gamma. \end{cases} \tag{9}$$

Similarly, to define the interface condition for the global pressure, let us introduce the jump function

$$j_p(\xi) = \begin{cases} \int_{s_{nr}^{(1)}}^{\xi} f_n^{(1)}(\pi^{(1)})' + P_e^{(1)} - P_e^{(2)}, & \text{if } \xi \in [s_{nr}^{(1)}, s^*), \\ \int_{s_{nr}^{(2)}}^{\bar{\pi}^{(2)}(\pi^{(1)}(\xi))} f_w^{(2)}(\pi^{(2)})' - \int_{s_{nr}^{(1)}}^{\xi} f_w^{(1)}(\pi^{(1)})', & \text{if } \xi \in [s^*, 1 - s_{wr}^{(1)}), \end{cases} \tag{10}$$

which is extended by the respective constants to provide continuity in $\mathbb{R}$. The interface conditions for the global pressure are (c.f.[14],[25]):

$$\begin{cases} \mathbf{q}^{(1)}(p^{(1)}, s^{(1)}) \cdot \eta_\Gamma = \mathbf{q}^{(2)}(p^{(2)}, s^{(2)}) \cdot \eta_\Gamma \quad \text{at } \Gamma \\ p^{(1)} - p^{(2)} = j_p(s^{(1)}) \quad \text{at } \Gamma. \end{cases} \tag{11}$$

Here the first condition imposes the continuity of the normal component of the flux $\mathbf{q}$ at the interface and the second prescribes the continuity of the wetting phase pressure, when the non-wetting phase is absent from one side of the interface, and the continuity of the non-wetting phase pressure, when the non-wetting phase is present in both media (c.f. [14]). In the definitions above, the jump of the global pressure, prescribed at the interface by (10), depends on the saturation value from one side of the interface only while its value from the another side is calculated (exactly) from the continuity of the capillary pressure. Observe that this formulation differs from the respective one used in [25] and provides more exact implementation of the interface conditions for the global pressure.

Depending on the physics of the considered model, different types of boundary conditions can be applied at the boundary of Ω, c.f [14]; we consider here the Dirichlet and Neumann type boundary conditions. Let us suppose that the boundary Ω is divided as $\partial\Omega = \partial\Omega_D \cup \partial\Omega_N$, where $\partial\Omega_D \neq \emptyset$ has a nonzero $(d-1)$ - dimensional measure and $\partial\Omega_D \cap \partial\Omega_N = \emptyset$. On the respective parts of the boundary $\partial\Omega$ the following boundary conditions are imposed:

$$\begin{cases} p = p_D, \quad s = s_D \quad \text{at } \partial\Omega_D \\ \mathbf{q}(p,s)\cdot\eta = 0, \quad \mathbf{r}(p,s;s)\cdot\eta = 0 \quad \text{at } \partial\Omega_N. \end{cases} \tag{12}$$

To close the formulation, we add the initial condition for saturation

$$s^{(\beta)} = s_0^{(\beta)} \quad \text{in } \Omega^{(\beta)},\ \beta = 1,2. \tag{13}$$

The existence of a weak solution to the problem (4),(12),(13) under assumptions 1 and 2 was proven in [13] for the Neumann type boundary conditions.

3. The sequential dG method

3.1. Time discretization

Let $\{t^m\}_{0\le m\le M}$ be a partition of time interval $[0,T]$ such that $t^0 = 0, t^M = T$, let $\tau_m = t^m - t^{m-1},\ m = 1,\dots,M$ be the time step and let $\tau = \max_{1\le m\le M}\tau_m$. For any vector space V of sufficiently smooth functions defined in Ω let us denote by $U_\tau^0(V) = \{u \in L^\infty((0,T),V) :\ u|_{(t^{m-1},t^m)} = u^m \in V\}$ the discretization space of $L^\infty((0,T),V)$ in time of order zero. Using implicit Euler timestepping, the sequential method for the time discretization of the system (4) is written as:

for a given $s^0 = s_0$ sequentially solve in Ω for $p^m, s^m,\ m = 1,\dots,M$ the following interface elliptic boundary value problems:

$$-\nabla\cdot\left(\kappa^{(\beta)}(s^{m-1})\nabla p^m\right) = (F_w^{(\beta)} + F_n^{(\beta)})^m \quad \text{in } \Omega^{(\beta)},\ \beta = 1,2; \tag{14}$$

$$\begin{cases} \mathbf{q}^{(1)}((p^{(1)})^m, (s^{(1)})^{m-1})\cdot\eta_\Gamma = \mathbf{q}^{(2)}((p^{(2)})^m, (s^{(2)})^{m-1})\cdot\eta_\Gamma \quad \text{at } \Gamma \\ (p^{(1)})^m - (p^{(2)})^m = j_p((s^{(1)})^{m-1}) \quad \text{at } \Gamma; \end{cases}$$

$$p^m = p_D^m \text{ at } \partial\Omega_D, \quad \mathbf{q}(p^m, s^{m-1})\cdot\eta = 0 \quad \text{at } \partial\Omega_N.$$

$$\nabla\cdot\left(-\epsilon^{(\beta)}(s^m)\nabla s^m + \mathbf{q}^{(\beta)}(p^m, s^{m-1}) f_n^{(\beta)}(s^m)\right) + \tau_m^{-1}\Phi^{(\beta)}s^m \tag{15}$$

$$= \tau_m^{-1}\Phi^{(\beta)}s^{m-1} + (F_n^{(\beta)})^m \quad \text{in } \Omega^{(\beta)},\ \beta = 1,2; \tag{16}$$

$$\begin{cases} \mathbf{r}^{(1)}((p^{(1)})^m, (s^{(1)})^{m-1}; (s^{(1)})^m)\cdot\eta_\Gamma = \mathbf{r}^{(2)}((p^{(2)})^m, (s^{(2)})^{m-1}; (s^{(2)})^m)\cdot\eta_\Gamma \quad \text{at } \Gamma \\ (s^{(1)})^m - (s^{(2)})^m = j_s((s^{(1)})^m) \quad \text{at } \Gamma; \end{cases}$$

$$s^m = s_D^m \text{ at } \partial\Omega_D, \quad \mathbf{r}(p^m, s^{m-1}; s^m)\cdot\eta = 0 \text{ at } \partial\Omega_N.$$

Note, that in contrast to that in [25], the scheme introduced here for the saturation equation is completely implicit in time including the diffusion term and the interface boundary condition.

3.2. dG space discretization

Let $\{\mathcal{T}_h\}_{h>0}$ be a family of shape-regular triangular meshes of the domain $\Omega \in \mathbb{R}^2$ (in the sequel for simplicity we will consider the two-dimensional case only). Let h_T be the diameter of element T and $h = \max_{T\in\mathcal{T}_h} h_T$ denotes the mesh size. Let $\mathcal{E}_h$ be the set of all edges of the mesh $\mathcal{T}_h$ and h_E denotes the diameter of edge E. We will suppose that the meshes are exactly fitted to the partition of Ω in subdomains and to the partition of $\partial\Omega$, corresponding to different boundary condition types; thus, we assume that $\Gamma, \partial\Omega_D$ and $\partial\Omega_N$ are exactly covered by edges from $\mathcal{E}_h$. We will denote the set of all edges covering $\partial\Omega_D, \partial\Omega_N$ and Γ by $\mathcal{E}_h^{\partial\mathrm{D}}, \mathcal{E}_h^{\partial\mathrm{N}}$ and $\mathcal{E}_h^{\Gamma}$ respectively. The set of all boundary edges will be denoted $\mathcal{E}_h^{\partial}$, so we have $\mathcal{E}_h^{\partial} = \mathcal{E}_h^{\partial\mathrm{D}} \cup \mathcal{E}_h^{\partial\mathrm{N}}$. We say that E is an interior edge of the mesh if E has a nonzero one-dimensional measure and if there are distinct $T^-, T^+ \subset \Omega^{(\beta)}$ in $\mathcal{T}_h$ such that $E = \partial T^- \cap \partial T^+$. The set of all interior edges is denoted by $\mathcal{E}_h^{\mathrm{i}}$; so the set of all edges is decomposed as $\mathcal{E}_h = \mathcal{E}_h^{\mathrm{i}} \cup \mathcal{E}_h^{\partial} \cup \mathcal{E}_h^{\Gamma}$.

Consider broken Sobolev space

$$H^s(\mathcal{T}_h) = \{u \in L^2(\Omega) | u \in H^s(T) \quad \forall T \in \mathcal{T}_h\}$$

with $s \geq 0$; here and in what follows we use standard notations from the Sobolev space theory, c.f. [1]. For any real function $v \in H^{\frac{1}{2}}(\mathcal{T}_h)$ let us denote the jump of v at $E \in \mathcal{E}_h^{\mathrm{i}} \cup \mathcal{E}_h^{\Gamma}$ by

$$[\![v]\!] := v^-|_E - v^+|_E, \qquad v^{\pm} := v|_{T^{\pm}},$$

and set for boundary edge $E \in \mathcal{E}_h^{\partial}$

$$[\![v]\!] = v|_E.$$

For $E \in \mathcal{E}_h^{\mathrm{i}}$, we define n_E as the unit normal vector to E pointing from T^- toward T^+, whereas for $E \in \mathcal{E}_h^{\partial}$ we set $n_E = \eta$ and for $E \in \mathcal{E}_h^{\Gamma}$ we set $n_E = \eta_\Gamma$. Note that the orientation of n_E for interior faces is chosen in accordance with the definition of the jump; in such a case the arbitrariness in the choice of T^- and T^+ is irrelevant.

Let us introduce for $E \in \mathcal{E}_h^{\mathrm{i}} \cup \mathcal{E}_h^{\Gamma}$ the standard arithmetic average of v at E by

$$\{\{v\}\} = \frac{v^-|_E + v^+|_E}{2}. \tag{17}$$

To cope with the discontinuity or degeneracy of diffusion coefficients in the elliptic part of the equations in system (4), we also introduce weighted averages as follows, c.f. [20, 27]. Consider a diffusion coefficient, say a, belonging to $H^1(\mathcal{T}_h)$. This coefficient can be two-valued on $E \in \mathcal{E}_h^{\mathrm{i}}$, so let us denote by $a_{T^-,E}$ and $a_{T^+,E}$ the values of a associated with T^- and T^+ respectively.

For all $E \in \mathcal{E}_h^{\mathrm{i}}$ such that $\|a_{T^-,E}\|_{L^\infty(E)} \cdot \|a_{T^+,E}\|_{L^\infty(E)} \neq 0$ we introduce the weights

$$\begin{aligned}
\omega_{T^-,E}(a) &= \frac{\|a_{T^+,E}\|_{L^\infty(E)}}{\|a_{T^-,E}\|_{L^\infty(E)} + \|a_{T^+,E}\|_{L^\infty(E)}}, \\
\omega_{T^+,E}(a) &= \frac{\|a_{T^-,E}\|_{L^\infty(E)}}{\|a_{T^-,E}\|_{L^\infty(E)} + \|a_{T^+,E}\|_{L^\infty(E)}},
\end{aligned} \tag{18}$$

such that $\omega_{T^-,E}(a)+\omega_{T^+,E}(a)=1$; the weighted average (in respect of a) of the function v is defined as

$$\{\{v\}\}_a = \omega_{T^-,E}(a)v^- + \omega_{T^+,E}(a)v^+. \tag{19}$$

We also denote the harmonic mean of a at E as

$$\langle a\rangle_E = \frac{2\|a_{T^-,E}\|_{L^\infty(E)}\|a_{T^+,E}\|_{L^\infty(E)}}{\|a_{T^-,E}\|_{L^\infty(E)}+\|a_{T^+,E}\|_{L^\infty(E)}}. \tag{20}$$

If $\|a_{T^-,E}\|_{L^\infty(E)}\cdot\|a_{T^+,E}\|_{L^\infty(E)}=0$ at $E\in\mathcal{E}_h^{\mathrm{i}}$ we set $\{\{v\}\}_a=\{\{v\}\}$ and $\langle a\rangle_E=\|a\|_{L^\infty(\Omega^{(\beta)})}$ if $E\in\Omega^{(\beta)}$. For $E\in\mathcal{E}_h^\Gamma$ we define $\{\{v\}\}_a=\{\{v\}\}$ and

$$\langle a\rangle_E = \frac{2\|a\|_{L^\infty(\Omega^{(1)})}\|a\|_{L^\infty(\Omega^{(2)})}}{\|a\|_{L^\infty(\Omega^{(1)})}+\|a\|_{L^\infty(\Omega^{(2)})}}. \tag{21}$$

The above definitions are extended to boundary edges E by setting $\{\{v\}\}_a=v$ and $\langle a\rangle_E=\|a\|_{L^\infty(\Omega^{(\beta)})}$ for $E\subset\partial T,\ T\subset\Omega^{(\beta)}$.

For a given order of polynomial approximation $k\geq 0$ we define the dG finite element space V_h^k as:

$$V_h^k := \{v_h\in L^2(\Omega);\ \forall T\in\mathcal{T}_h,\ v_h|_T\in\mathbb{P}_k(T)\}, \tag{22}$$

where $\mathbb{P}_k(T)$ denotes the vector space of polynomials with total degree $\leq k$ on T. Also, let us denote by $U_\tau^0(V_h^k)$ the respective time discretization space.

Given $s_h^{m-1}\in V_h^k, 1\leq m\leq M$ from the previous time step ($m\geq 1$) we solve the pressure equation (14) using the interior penalty dG method, that is, we solve for $p_h^m\in V_h^k$ such that $\forall v_h\in V_h^k$,

$$\begin{aligned}
&\sum_{T\in\mathcal{T}_h}\int_T \kappa(s_h^{m-1})\nabla p_h^m\cdot\nabla v_h \\
&-\sum_{E\in\mathcal{E}_h^{\mathrm{i}}\cup\mathcal{E}_h^{\partial\mathrm{D}}}\int_E\Big(\{\{n_E\cdot\kappa(s_h^{m-1})\nabla p_h^m\}\}_{\kappa(s_h^{m-1})}[\![v_h]\!]+\vartheta\{\{n_E\cdot\kappa(s_h^{m-1})\nabla v_h\}\}_{\kappa(s_h^{m-1})}[\![p_h^m]\!]\Big) \\
&+\sum_{E\in\mathcal{E}_h^{\mathrm{i}}\cup\mathcal{E}_h^{\partial\mathrm{D}}}\langle\kappa(s_h^{m-1})\rangle_E\frac{\sigma_E k^2}{h_E}\int_E[\![p_h^m]\!][\![v_h]\!]=\sum_{T\in\mathcal{T}_h}\int_T\left(F_w^m+F_n^m\right)v_h \\
&+\sum_{E\in\mathcal{E}_h^\Gamma}\int_E\left(-\vartheta\{\{n_E\cdot\kappa(s_h^{m-1})\nabla v_h\}\}_{\kappa(s_h^{m-1})}+\langle\kappa(s_h^{m-1})\rangle_E\frac{\sigma_E k^2}{h_E}[\![v_h]\!]\right)j_p(\chi_E^{(1)}(s_h^{m-1})) \\
&+\sum_{E\in\mathcal{E}_h^{\partial\mathrm{D}}}\int_E\left(-\vartheta n_E\cdot\kappa(s_h^{m-1})\nabla v_h+\langle\kappa(s_h^{m-1})\rangle_E\frac{\sigma_E k^2}{h_E}v_h\right)p_D^m.
\end{aligned} \tag{23}$$

Here the method parameter $\vartheta=1$ corresponds to the symmetric version and $\vartheta=-1$ corresponds to the non-symmetric version of dG, σ_E is a mesh dependent parameter and for $E\in\mathcal{E}_h^\Gamma,\ E=\overline{T^-}\cap\overline{T^+}$ the functional $\chi_E^{(1)}$ on V_h^k is defined by

$$\chi_E^{(1)}(v_h)=\begin{cases} v_h^-|_E, & \text{if } T^-\subset\Omega^{(1)},\\ v_h^+|_E, & \text{if } T^+\subset\Omega^{(1)}.\end{cases} \tag{24}$$

The approximate pressure p_h^m has been computed in V_h^k, so the normal component of $\mathbf{q}_h^m = \kappa^{(\beta)}(s^{m-1})\nabla p^m$, locally defined in each element T, can not be continuous at the faces $E \in \mathcal{E}_h^{\mathrm{i}} \cup \mathcal{E}_h^{\Gamma}$. To correct this, we use the reconstruction operator $\mathcal{R}_0 : V_h^k \times V_h^k \to \mathbf{RT}_0(\mathcal{T}_h)$, introduced in [25] in more general setting, that projects $\mathbf{q}_h$ in the lowest-order Raviart-Thomas-Nédélec finite element space

$$\mathbf{RT}_0(\mathcal{T}_h) = \{u_h \in \mathbf{H}(div); \forall T \in \mathcal{T}_h, u_h|T \in [\mathbb{P}_0(T)]^d + \mathbf{x}\mathbb{P}_0(T)\}. \tag{25}$$

The reconstructed flux $\mathbf{u}_h^m = \mathcal{R}_0\mathbf{q}_h^m$ has continuous normal component at all interior faces and at the interface, that is satisfies the first interface condition in (14). Moreover, the divergence of the reconstructed flux is optimal, i.e. the next equality is valid $\nabla \cdot \mathbf{u}_h^m = \Pi_h^1(F_w^m + F_n^m)$, where Π_h^k is the L^2 projector on V_h^k. In the lowest-order Raviart-Thomas-Nédélec space the local degrees of freedom of u_h^m are easily calculated from the equations

$$\begin{aligned}
\int_E (\mathbf{u}_h^m \cdot n_E) &= \int_E \left(-n_E \cdot \{\{\kappa(s_h^{m-1})\nabla p_h^m\}\}_{\kappa(s_h^{m-1})} + \langle \kappa(s_h^{m-1})\rangle_E \frac{\sigma_E k^2}{h_E} [\![p_h^m]\!]' \right), \\
&\qquad\qquad \forall E \in \mathcal{E}_h \setminus \mathcal{E}_h^{\partial \mathrm{N}}; \qquad (26) \\
\int_E (\mathbf{u}_h^m \cdot n_E) &= 0 \quad \forall E \in \mathcal{E}_h^{\partial \mathrm{N}};
\end{aligned}$$

where $[\![\cdot]\!]'$ is defined by

$$[\![p_h^m]\!]' = \begin{cases} [\![p_h^m]\!], & \text{se } E \in \mathcal{E}_h^{\mathrm{i}}, \\ [\![p_h^m]\!] - j_p(\chi_E^1(s_h^{m-1})), & \text{se } E \in \mathcal{E}_h^{\Gamma}, \\ p_h^m - p_D, & \text{se } E \in \mathcal{E}_h^{\partial \mathrm{D}}. \end{cases}$$

Let us consider standard edge-oriented basis $\{\psi_E | E \in \mathcal{E}_h\}$ of $\mathbf{RT}_0(\mathcal{T}_h)$ (see e.g. [23]) such that $(\psi_E \cdot n_E)|_{E'} = \delta_{E,E'} \quad \forall E, E' \in \mathcal{E}_h$, and let $\mathbf{u}_h^m = \sum_{E \in \mathcal{E}_h} u_E^{h,m} \psi_E$ be the representation of $\mathbf{u}_h^m$ with respect to this basis. Then the system (26) is recast into the diagonal system for the unknown ψ_E that has the solution

$$\begin{aligned}
u_E^{h,m} &= \int_E \left(-n_E \cdot \{\{\kappa(s_h^{m-1})\nabla p_h^m\}\}_{\kappa(s_h^{m-1})} + \langle \kappa(s_h^{m-1})\rangle_E \frac{\sigma_E k^2}{h_E} [\![p_h^m]\!]' \right), \\
&\qquad\qquad \forall E \in \mathcal{E}_h \setminus \mathcal{E}_h^{\partial \mathrm{N}}; \\
u_E^{h,m} &= 0 \quad \forall E \in \mathcal{E}_h^{\partial \mathrm{N}}.
\end{aligned}$$

Consequently the reconstruction procedure can be performed edgewise and demands the minimal computational effort.

Next we solve numerically the saturation equation (15) using the interior penalty dG method for approximation of the diffusion term and the dG method with Godunov numerical flux for the nonlinear advective term. For a given $p_h^m \in V_h^k$ and $\mathbf{u}_h^m \in \mathbf{RT}_0(\mathcal{T}_h)$ we solve for

$s_h^m \in V_h^k$ such that for all $z_h \in V_h^k$,

$$
\begin{aligned}
&\sum_{T\in\mathcal{T}_h}\int_T \epsilon(s_h^m)\nabla s_h^m\cdot\nabla z_h \\
&-\sum_{E\in\mathcal{E}_h^{\mathrm{i}}\cup\mathcal{E}_h^{\partial\mathrm{D}}}\int_E\Big(\{\{n_E\cdot\epsilon(s_h^m)\nabla s_h^m\}\}_{\epsilon(s_h^{m-1})}[\![z_h]\!]+\vartheta\{\{n_E\cdot\epsilon(s_h^m)\nabla z_h\}\}_{\epsilon(s_h^{m-1})}[\![s_h^m]\!]\Big) \\
&+\sum_{E\in\mathcal{E}_h^{\mathrm{i}}\cup\mathcal{E}_h^{\partial\mathrm{D}}}\langle\epsilon(s_h^{m-1})\rangle_E\frac{\sigma_E k^2}{h_E}\int_E[\![s_h^m]\!][\![z_h]\!]+\sum_{T\in\mathcal{T}_h}\int_T\tau_m^{-1}\Phi s_h^m z_h \\
&-\sum_{T\in\mathcal{T}_h}\int_T\mathbf{u}_h^m f_n(s_h^m)\cdot\nabla z_h+\sum_{E\in\mathcal{E}_h}\int_E(\mathbf{u}_h^m\cdot n_E)\Psi_{hE}^m[\![z_h]\!] \\
&+\sum_{E\in\mathcal{E}_h^{\Gamma}}\int_E\left(\vartheta\{\{n_E\cdot\epsilon(s_h^m)\nabla z_h\}\}_{\epsilon(s_h^{m-1})}-\langle\epsilon(s_h^{m-1})\rangle_E\frac{\sigma_E k^2}{h_E}[\![z_h]\!]\right)j_s(\chi_E^{(1)}(s_h^m)) \\
&+\sum_{E\in\mathcal{E}_h^{\partial\mathrm{D}}}\int_E\vartheta n_E\cdot\epsilon(s_h^m)\nabla z_h s_D^m=\sum_{T\in\mathcal{T}_h}\int_T\tau_m^{-1}\Phi s_h^{m-1}z_h \\
&+\sum_{T\in\mathcal{T}_h}\int_T F_n^m z_h+\sum_{E\in\mathcal{E}_h^{\partial\mathrm{D}}}\int_E\langle\epsilon(s_h^{m-1})\rangle_E\frac{\sigma_E k^2}{h_E}z_h s_D^m
\end{aligned}
\tag{27}
$$

The numerical flux of the Godunov type Ψ_{hE}^m is defined as

$$
\Psi_{hE}^m=\begin{cases}f_n(s_h^{m,\uparrow}) & \text{if } E\in\mathcal{E}_h^{\mathrm{i}},\\ \{\{f_n(s_h^m)\}\} & \text{if } F\in\mathcal{E}_h^{\Gamma},\\ f_n(s_h^m) & \text{if } E\in\mathcal{E}_h^{\partial\mathrm{N}},\\ f_n(s_D^m) & \text{if } F\in\mathcal{E}_h^{\partial\mathrm{D}},\end{cases}
\tag{28}
$$

where $s_h^{m,\uparrow}$ denotes the upwind value of s_h^m.

To resolve the nonlinear system we utilize the Newton-like method using the Picard linearization for the diffusion term and the Newton linearization for the advective term of the saturation equation. More exactly, let $\{\psi_n\}, n=1,\dots,N=\dim V_h^k$ be a basis of V_h^k and let $u_h^m\in\mathbb{R}^N$ be the representation of the saturation s_h^m at a time step m with respect to this basis. Non-linear system (27) can be rewritten as $A(u_h^m)u_h^m=f^m$, where A is the global stiffness matrix and f^m is the load vector. Let us decompose $A(u)=D(u)+C(u)$, where D includes the terms corresponding to the diffusion operator and the interface condition while the terms of the advective part are collected in C. Denote by $J_{\mathcal{C}}$ the Jacobian of non-linear function $\mathcal{C}(u)=C(u)u,\quad \mathcal{C}:\mathbb{R}^N\to\mathbb{R}^N$. The Newton-like scheme for the non-linear system is:

for a given $1\le m\le M$, $u_h^{m,0}=u_h^{m-1}$, solve for $u_h^{m,i}\in\mathbb{R}^N,\ i=1,\dots,I_{\max}$,

$$
D(u_h^{m,i-1})u_h^{m,i}+J_{\mathcal{C}}(u_h^{m,i-1})(u_h^{m,i}-u_h^{m,i-1})=-\mathcal{C}(u_h^{m,i-1})+f^m
$$

and go to the next time step if $\|u_h^{m,i} - u_h^{m,i-1}\|_{L^2(\Omega)} < \delta_{tol}$, where δ_{tol} is a prescribed tolerance value and $I_{\max}$ is a maximum iteration number.

This scheme is simpler than the Newton method and is more appropriate to convection dominated problems. In comparison with [25], where the diffusion terms and the interface condition were linearized by freezing at the previous time step, a more robust and faster converging solution procedure can be expected.

4. Numerical results

For numerical validation of the dG method presented in the previous section we consider four two-dimensional test cases. The first one aims to examine the convergence order of the dG method for a non-linear degenerate parabolic equation with linear advection. The second one assesses the dG method in the synthetic problem for a coupled system of pressure - saturation equation, that admits an exact solution, and investigates the effects of the accuracy of total velocity reconstruction on the convergence order for a coupled system. The third test case aims to analyze the accuracy of the implementation of the non-linear interface condition using the dG penalty technique described above. In the fourth test case we demonstrate the potential of the proposed dG method considering the numerical simulation of the heterogeneous five-spot problem with different rock types in the presence of capillary barriers.

In all test cases we use the symmetric version of the the sequential interior penalty dG method. For stability of the symmetric method, the size of the penalty parameter has to be large enough, see e.g. [19]. The minimal value of the penalty parameter depends on the value of the constant from the inverse trace inequality and the mesh regularity; its evaluation is a non-trivial task even for linear elliptic equation. In presented simulations we use the value $\sigma_E = 10$ that was observed to be large enough to guarantee stability of the method.

The numerical simulations have been performed using developed by authors MATLAB software package that implements discontinuous Galerkin method in two-dimensional geometry in fast sparse matrix programming environment. For mesh management we use the data structure and algorithms from iFEM MATLAB package [15] containing robust and efficient codes for unstructured simplicial grids. Standard MATLAB's sparse matrix utilities, including built-in backslash operator that uses UMFPACK package for sparse multifrontal LU factorization [18], are employed for solving linear systems.

4.1. Test case 1

In $\Omega = (0,1)^2$ consider the initial boundary value problem for the non-linear degenerate diffusion - advection equation

$$\begin{aligned} &\partial_t u + \nabla \cdot (-\epsilon(u)\nabla u + \mathbf{q} f(u)) = F, \\ &u|_{\partial\Omega} = 0, \\ &u|_{t=0} = u_0, \end{aligned} \tag{29}$$

where $f(u) = u, \epsilon(u) = 2\nu u, \mathbf{q} = (1,1)$ and F, u_0 are such that

$$u(x,t) = (e^t - 1)x_1 x_2 \tanh\left(\frac{1-x_1}{0.2}\right)\tanh\left(\frac{1-x_2}{0.2}\right)$$

is the exact solution to the problem. For $\nu = 0.1$ we solve numerically the problem (29) at the nested sequence of the uniform structured triangular meshes using a uniform sufficiently small time step $\tau = 5\times 10^{-3}$ on the time interval $(0,1)$ to guarantee a dominance of the space approximation error. Let u_h denote the approximate solution at time $t = 1$, k denote the order of polynomial approximation and h denote the diameter of the mesh. Below for orders of approximation $k = 1, 2$ we present the convergence orders of the implicit dG method, introduced for the saturation equation in Section 3 (Table 1). As the convergence criterion in the Newton-like method we use a tolerance of 10^{-12} in the $L^2(\Omega)$ norm. We observe that the implicit dG method exhibits optimal orders of the convergence for the considered approximation orders.

k	h	$\|u - u_h\|_{L^2(\Omega)}$	Conv. order	$\|\nabla u - \nabla_h u_h\|_{L^2(\Omega)}$	Conv. order
	0.35	3.5472e-2		7.8450e-1	
1	0.18	1.0587e-2	1.7444	4.4422e-1	0.8205
	0.088	2.5152e-3	2.0735	2.2333e-1	0.9921
	0.044	6.1060e-4	2.0424	1.1017e-1	1.0194
	0.35	6.8491e-3		2.4800e-1	
2	0.18	1.0655e-3	2.6844	6.6036e-2	1.9090
	0.088	1.4240e-4	2.9035	1.6112e-2	2.0351
	0.044	1.8343e-5	2.9566	4.0417e-3	1.9951

Table 1: Implicit dG method: errors and convergence orders at $t = 1$ for test case 1.

4.2. Test case 2

Following [41], consider in $\Omega = (0,1)^2$ the benchmark problem given below:

$$\begin{aligned} &\nabla\cdot(\kappa(s)\nabla p) = 0, \\ &\mathbf{q} = \kappa(s)\nabla p, \\ &\partial_t s + \nabla\cdot(-\epsilon\nabla s + \mathbf{q}f(s)) = F, \end{aligned} \tag{30}$$

with $\kappa(s) = (0.5 - 0.2s)^{-1}, \epsilon = 0.01, f(s) = s$, where $F = 2\pi^2\epsilon\sin(\pi(x_1 + x_2 - 2t))$, boundary and initial conditions correspond to the exact solution

$$\begin{aligned} p &= \frac{0.2}{\pi}\cos(\pi(x_1 + x_2 - 2t)) + 0.5(x_1 + x_2), \\ s &= \sin(\pi(x_1 + x_2 - 2t)). \end{aligned}$$

In Tables 2 and 3 the errors and convergence orders of first order dG, calculated on nested sequences of structured triangular meshes, are presented for pressure, total velocity

and saturation at final time $T = 0.2$. In the simulation a small uniform time step was used to eliminate time error pollution. We can observe that the convergence order is optimal for all three variables.

h	$\|p - p_h\|_{L^2}$	Conv.ord.	$\|\nabla p - \nabla_h p_h\|_{L^2}$	Conv.ord.	$\|\mathbf{q} - \mathbf{q}_h\|_{L^2\times L^2}$	Conv.ord.
0.35	3.4454e-3	2.0182	6.3955e-2	1.1928	2.5046e-2	1.8927
0.18	9.0223e-4	1.9331	3.2005e-2	0.9988	6.3191e-3	1.9868
0.088	2.2732e-4	1.9888	1.5934e-2	1.0062	1.5999e-3	1.9817
0.044	5.7361e-5	1.9866	7.9442e-3	1.0041	4.2322e-4	1.9185

Table 2: Errors and convergence orders of dG method for pressure and reconstructed total velocity at $T = 0.2$ for first order of approximation; $\tau = 3.1250 \times 10^{-5}$ was used, which corresponds to 6400 time steps.

h	$\|s - s_h\|_{L(2)}$	Conv. ord.	$\|\nabla s - \nabla_h s_h\|_{L(2)}$	Conv. ord.
0.35	4.0669e-2	1.7523	1.0058e+0	0.5907
0.18	9.8238e-3	2.0496	5.0519e-1	0.9934
0.088	2.3300e-3	2.0760	2.4628e-1	1.0365
0.044	5.6721e-4	2.0384	1.1982e-1	1.0394

Table 3: Errors and convergence orders of dG method for saturation at $T = 0.2$ for first order of approximation; $\tau = 3.1250 \times 10^{-5}$ was used, which corresponds to 6400 time steps

4.3. Test case 3

Here we consider the two-dimensional extension of the interface problem, for which a one dimensional quasi analytical solution is available [44]. Consider the domain $\Omega = (-0.6, 0.6)^2$ divided into the two subdomains $\Omega^{(1)} = (-0.6, 0) \times (-0.6, 0.6)$, $\Omega^{(2)} = (0, 0.6) \times (-0.6, 0.6)$ by interface $\Gamma = \{(0, y) : \ y \in (-0.6, 0.6)\}$. The evolution problem for the degenerate parabolic equation is

$$
\begin{aligned}
&\Phi^\beta \partial_t s^\beta - \nabla \left(\epsilon^\beta(s^\beta)\nabla s^\beta\right) = 0, \quad (x, y, t) \in \Omega^{(\beta)} \times (0, T), \beta \in \{1, 2\},\\
&s(-0.6, y, t) = 0, \quad s(0.6, y, t) = 1, \quad y \in (-0.6, 0.6), t \in (0, T),\\
&\partial_y s(x, -0.6, t) = \partial_y s(x, 0.6, t) = 0, \quad x \in (-0.6, 0.6), t \in (0, T),\\
&\epsilon^{(1)}(s^{(1)})\partial_x s^{(1)}|_\Gamma = \epsilon^{(2)}(s^{(2)})\partial_x s^{(2)}|_\Gamma, \quad [\![s]\!]|_\Gamma = j_s(s^{(1)}), t \in (0, T)\\
&s(x, y, 0) = \begin{cases} 0 & \text{if } x \in (-0.6, 0),\\ 1 & \text{if } x \in (0, 0.6). \end{cases}
\end{aligned}
\tag{31}
$$

We use the Brooks-Corey model [5] for relative permeability and capillary pressure

$$
\begin{aligned}
kr_w^{(\beta)} &= (1 - s_{ne}^{(\beta)})^{(2+3\theta^{(\beta)})/\theta^{(\beta)}},\\
kr_n^{(\beta)} &= (s_{ne}^{(\beta)})^2(1 - (1 - s_{ne}^{(\beta)})^{(2+\theta^{(\beta)})/\theta^{(\beta)}}),\\
\pi &= P_e^{(\beta)}(1 - s_{ne}^{(\beta)})^{-1/\theta^{(\beta)}},
\end{aligned}
$$

with entry pressure $P_e^{(\beta)} = (\Phi^{(\beta)}/K^{(\beta)})^{1/2}$. The parameters values for the porous medium corresponding to example in [44] are presented in Table 4, where the columns contain two values, one for each subdomain. Here we consider two test cases TC3a and TC3b; in both of them the porous medium occupying the subdomain $\Omega^{(2)}$ has a finer texture while the jump of the permeability at the interface is larger in TC3b. In both test cases we consider $\mu_w = \mu_n = 1$. Note, that owing to the different values of the jump of the permeability in considered test cases, the solution exhibits different type of discontinuity at the interface for $t = 1$, see Figures 1 and 2. In the first test case the threshold saturation is $s^* \approx 0.36$ and $s^{(1)} \approx 0.58 > s^*$, so the capillary pressure is continuous at the interface, see (8). In the second one $s^* \approx 0.75$ and $s^{(1)} \approx 0.54 < s^*$, so the capillary pressure is discontinuous at the interface.

Porous medium			
Par.	Value	Par.	Value
Φ	$(1, 1)$	θ	$(2, 2)$
K	$(1, 0.64)$ (TC3a)	s_{nr}	$(0, 0)$
K	$(1, 0.25)$ (TC3b)	s_{wr}	$(0, 0)$

Table 4: Parameter values for the porous medium used in test case 3a and 3b.

Below we present examples of two numerical experiments for test case 3a and test case 3b respectively. For the simulation time $t = 1$ we compare the restriction to $y = 0$ of the numerical two-dimensional solution, calculated by the present method, with the one-dimensional self-similar solution from [44] for different mesh sizes, time steps and polynomial orders of approximation. In absence of the adjective term, Newton-like method, used for solution of the non-linear system, reduces to the fixed point (Picard) iteration (dGfp). The objective of this test is to study the efficiency of the dG method with fixed point iteration (dGfp) in resolving the non-linearity of the diffusion term and interface condition in comparison with the linearization from the previous time step (dGl) used in [25].

Figures 1 and 2 present the results for test cases 3a and 3b, respectively, where following [44], we plot the wetting phase saturation profiles. Mesh parameters and order of approximation are indicated in figure captions, the stopping error 10^{-4} in the $L^2(\Omega)$ norm was used in the Picard iteration. The approximate solution converges to the exact solution in all cases, but the implicit dGfp method converges faster even on moderately refined meshes while the dGl method still exhibits a visible error even on the finest mesh. Although the discontinuity of the saturation at the interface seems to be well captured by both methods, the delay of the saturation front of the approximate solution of the dGl method could be caused by imposing the value of the saturation jump on the interface from the previous time step.

4.4. Heterogeneous five-spot problem

In this test case we consider the heterogeneous five-spot problem with the geometric configuration presented in the Figure 3(a). The domain is divided into two subdomains $\Omega^{(2)} = (93.75, 206.25)\times(93.75, 206.25)$ and $\Omega^{(1)} = \Omega\backslash\bar{\Omega}^{(2)}$ with the porous medium properties

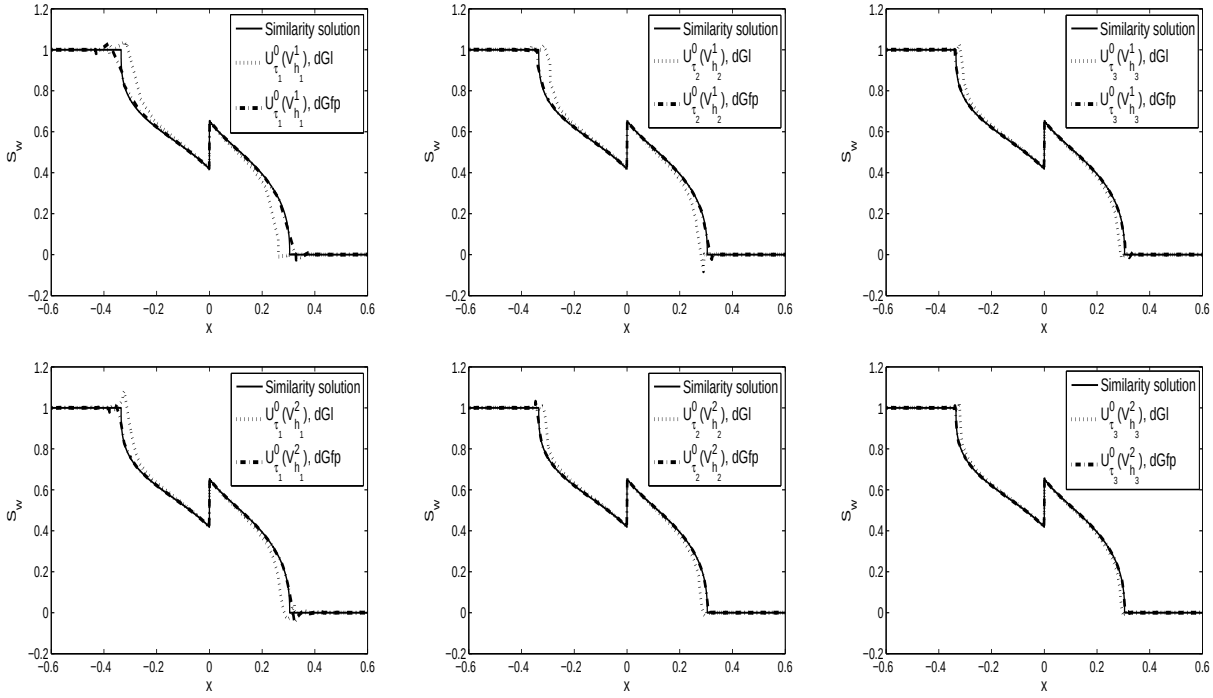

Figure 1: Test case 3a. Wetting phase saturation calculated in space $U^0_{\tau_i}(V^1_{h_i})$ with $\tau_1 = 5 \times 10^{-2}, h_1 = 9.5 \times 10^{-2}, \tau_2 = 2.5 \times 10^{-2}, h_2 = 5.4 \times 10^{-2}, \tau_3 = 1.25 \times 10^{-2}, h_3 = 3.2 \times 10^{-2}$ (first line, from left to right) and in space $U^0_{\tau_i}(V^2_{h_i})$ with $\tau_1 = 2.5 \times 10^{-2}, h_1 = 9.5 \times 10^{-2}, \tau_2 = 1.25 \times 10^{-2}, h_2 = 5.4 \times 10^{-2}, \tau_3 = 6.25 \times 10^{-3}, h_3 = 3.2 \times 10^{-2}$ (second line, from left to right) using the dGl and dGfp methods in comparison with the similarity solution from [44].

defined in Table 5 for two test cases TC4a and TC4b respectively. Here the Brooks-Corey model [5] is used for relative permeability and capillary pressure. We consider an oil as the non-wetting fluid with viscosity $\mu_n = 0.01\ kg/m\ s$ and water as the wetting fluid with viscosity $\mu_w = 0.001\ kg/m\ s$. Initially the oil blob is placed in Ω_{oil} (see Figure 3(b)) while the rest of Ω is saturated by water. Water is injected along the boundary $\partial\Omega^-$ and fluid is pushed out through the boundary $\partial\Omega^+$; no flow boundary condition is assumed on the rest of the boundary. Thus, the boundary and initial conditions are given by

$$\begin{aligned} -\eta \cdot \mathbf{q}_n^{(1)}|_{\partial\Omega^-} &= 0, \quad -\eta \cdot \mathbf{q}_w^{(1)}|_{\partial\Omega^-} = 7 \times 10^{-6} m/s; \\ p|_{\partial\Omega^+} &= 1.16 \times 10^5\ Pa, \quad s|_{\partial\Omega^+} = 0; \\ -\eta \cdot \mathbf{q}^{(1)}|_{\partial\Omega_N} &= 0, \quad -\eta \cdot \mathbf{q}_w^{(1)}|_{\partial\Omega_N} = 0; \\ s_0(x,y,0) &= \begin{cases} 0.8 & \text{if}(x,y) \in \Omega_{oil}, \\ 0 & \text{otherwise.} \end{cases} \end{aligned}$$

Here $\mathbf{q}_\alpha^{(\beta)} = -\kappa^{(\beta)} \nabla p_\alpha$ denotes volumetric flux of the phase α in $\Omega^{(\beta)}$ and the global pressure prescribed at Ω^+ corresponds to the wetting pressure value $p_w = 10^5\ Pa$. The objective

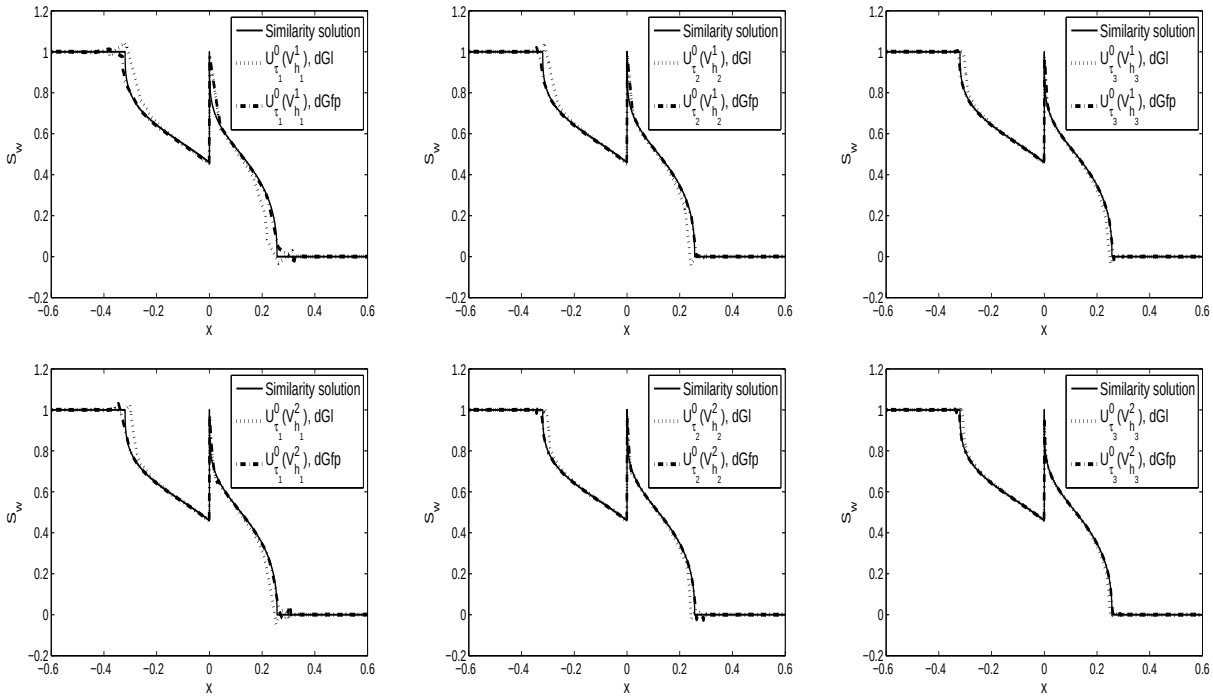

Figure 2: Test case 3b. Wetting phase saturation calculated in space $U^0_{\tau_i}(V^1_{h_i})$ with $\tau_1 = 5 \times 10^{-2}, h_1 = 9.5 \times 10^{-2}, \tau_2 = 2.5 \times 10^{-2}, h_2 = 5.4 \times 10^{-2}, \tau_3 = 1.25 \times 10^{-2}, h_3 = 3.2 \times 10^{-2}$ (first line, from left to right) and in space $U^0_{\tau_i}(V^2_{h_i})$ with $\tau_1 = 2.5 \times 10^{-2}, h_1 = 9.5 \times 10^{-2}, \tau_2 = 1.25 \times 10^{-2}, h_2 = 5.4 \times 10^{-2}, \tau_3 = 6.25 \times 10^{-3}, h_3 = 3.2 \times 10^{-2}$ (second line, from left to right) using the dGl and dGfp methods in comparison with the similarity solution from [44].

of these two tests is to study the propagation of the oil blobs in the heterogeneous domain with different capillary pressure forces.

For the simulation we generate two non-uniform triangular meshes $\mathcal{T}_h^{(a)}$ and $\mathcal{T}_h^{(b)}$ for test cases 4a and 4b respectively; both meshes are presented in Figure 4. The quality of the mesh $\mathcal{T}_h$ is evaluated as (see e.g. [32])

$$\bar{q}(\mathcal{T}_h) = \frac{1}{\#(\mathcal{T}_h)} \sum_{T \in \mathcal{T}_h} q(T), \quad q(T) = 2\frac{\rho(T)}{r(T)},$$

where $\rho(T)$ is the radius of the inscribed circle and $r(T)$ is the radius of the circumscribed circle; note that an equilateral triangle T has $q(T) = 1$. For the meshes considered we have $\bar{q}(\mathcal{T}_h^{(a)}) = \bar{q}(\mathcal{T}_h^{(b)}) = 0.95$. Below in Figures 5-6 we present the results of the simulations for test case TC4a and TC4b respectively. We use the implicit sequential dG method described above with the first order of approximation for the pressure and the saturation and with total velocity reconstruction in the lowest-order Raviart-Thomas-Nédélec finite element space. The stopping error in the Newton-like method is 10^{-8} in the $L^2(\Omega)$ norm. The additional isotropic diffusion stabilization in the saturation equation (see [9]) was used to remedy overshoots or undershoots near sharp fronts (interface).

In test case 4a (Figure 5) initially the oil is pushed by the water in the diagonal direction until reaching the interface at time $t \approx 70$ days. Next oil preferentially enters $\Omega^{(2)}$ which has higher permeability through the inflow part of the interface stimulated by a "sucking" effect owing to a difference in the entry pressures as observed from the respective vector plots of the total velocity field. At approximately 350 days oil arrives at the outflow part of the interface and is stopped here while the saturation reaches threshold saturation $s^* = 0.6$ at $t \approx 725$ days firstly in the bottom right corner of $\Omega^{(2)}$. Next the oil crosses the interface and enters $\Omega^{(1)}$ forming the "finger" in the diagonal direction; the oil front in $\Omega^{(1)}$ that get around $\Omega^{(2)}$ is delayed owing to a lower permeability of the rock and the finger reaches the production well at $t \approx 1800$ days.

In test case 4b, in contrast to the previous test case, $\Omega^{(2)}$ is less permeable and has a higher entry pressure, so when the oil reaches the interface at $t \approx 2$ days, it preferentially gets around $\Omega^{(2)}$ since to enter in this sub-domain the pressure must surpass the entry pressure. When this occurs at $t \approx 60$ days, only small fraction of the oil enters $\Omega^{(2)}$. At $t \approx 950$ days the oil completely turn out $\Omega^{(2)}$ and reaches the production well at $t \approx 2970$ days.

From this test case we can conclude that contrast discontinuous permeability and capillary pressure barriers, depending on geometry of heterogeneities in simulated petroleum reservoir, can significantly influence on the secondary oil recovery process, in particular on the arrival time.

Test Case 4a		Test Case 4b	
Par.	Value	Par.	Value
Φ	$(0.2, 0.2)$ (-)	Φ	$(0.2, 0.2)$ (-)
K	$(10^{-12}, 10^{-10})$ m$^{(2)}$	K	$(10^{-10}, 10^{-11})$ m$^{(2)}$
P_e	$(1.58 \times 10^4, 1 \times 10^4)$ Pa	P_e	$(1 \times 10^4, 1.58 \times 10^4)$ Pa
θ	$(2, 2)$ (-)	θ	$(2, 2)$ (-)
s_{nr}	$(0, 0)$ (-)	s_{nr}	$(0, 0)$ (-)
s_{wr}	$(0, 0)$ (-)	s_{wr}	$(0, 0)$ (-)

Table 5: Parameter values for the porous medium used in test case 4.

Acknowledgment. The authors thank the unknown referees for a number of helpful suggestions and useful comments.

[1] R. A. Adams. *Sobolev Spaces*. Academic Press, 1975.

[2] B. Amaziane, A. Bourgeat, and H. El Amri. Existence of solutions to various rock types model of two-phase flow in porous media. *Appl. Anal.*, 60(1-2):121–132, 1996.

[3] P. Bastian and R. Béatrice. Superconvergence and H(div) projection for discontinuous Galerkin methods. *Internat. J. Numer. Methods Fluids.*, 42(10):1043–1057, 2003.

[4] P. Bastian and B. Rivière. Discontinuous Galerkin methods for two-phase flow in porous media. *Technical Report 2004-28*, 2004.

[5] J. Bear. *Dynamic of Fluids in Porous Media*. Dover, New York, New York, 1978.

[6] M. Bertsch, R. Dal Passo, and C. Van Duijn. Analysis of oil trapping in porous media flow. *SIAM J. Math. Anal.*, 35:245–267, 2003.

[7] A. Bourgeat and A. Hidani. Effective model of two-phase flow in a porous medium made of different rock types. *Appl. Anal.*, 58(1-2):1–29, 1995.

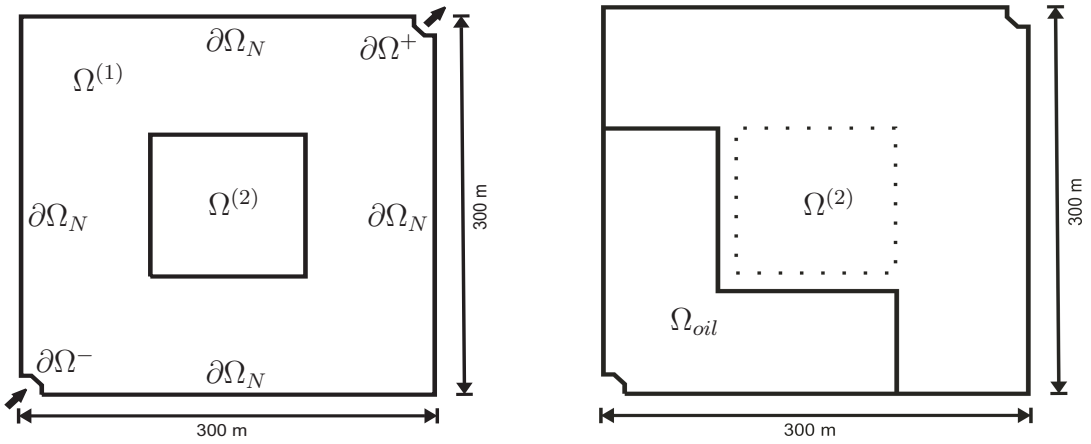

Figure 3: (a)Heterogeneous five-spot geometry. (b) Initial position of the boil of oil.

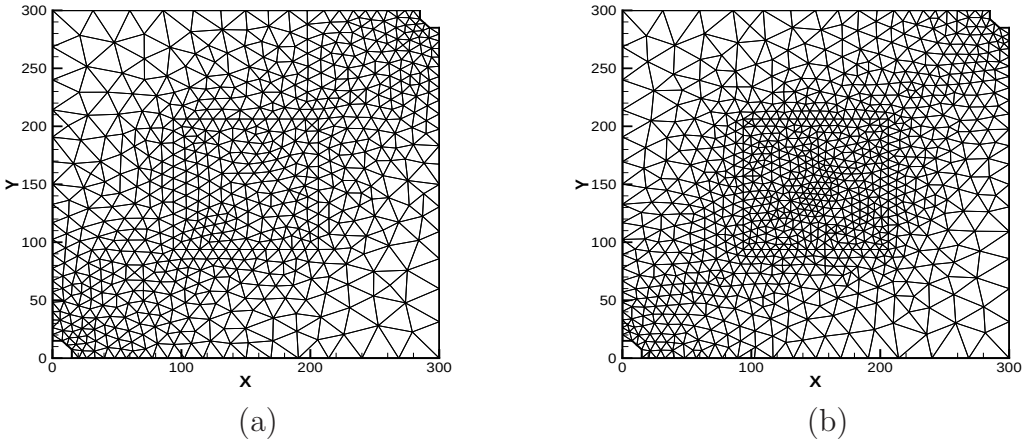

Figure 4: (a) Mesh $\mathcal{T}_h^{(a)}$ used in TC4a, 1296 elements. (b) Mesh $\mathcal{T}_h^{(b)}$ used in TC4b, 1840 elements.

[8] K. Brenner, C. Cancès, and D. Hilhorst. Finite volume approximation for an immiscible two-phase flow in porous media with discontinuous capillary pressure. HAL-00675681, Sept. 2011.

[9] E. Burman and A. Ern. Nonlinear diffusion and discrete maximum principle for stabilized Galerkin approximations of the convection–diffusion-reaction equation. *Comput. Methods Appl. Mech. Engrg.*, 191(35):3833–3855, 2002.

[10] F. Buzzi, M. Lenzinger, and B. Schweizer. Interface conditions for degenerate two-phase flow equations in one space dimension. *Analysis (Munich)*, 29(3):299–316, 2009.

[11] C. Cancès. Finite volume scheme for two-phase flow in heterogeneous porous media involving capillary pressure discontinuities. *M2AN Math. Model. Numer. Anal.*, 43:973–1001, 2009.

[12] C. Cancès, T. Gallout, and A. Porretta. Two-phase flows involving capillary barriers in heterogeneous porous media. *Interfaces and Free Boundaries*, 11:239–258, 2009.

[13] C. Cancès and M. Pierre. An existence result for multidimensional immiscible two-phase flows with discontinuous capillary pressure field. Technical report, HAL : hal-00518219, 2011.

[14] G. Chavent and J. Jaffré. *Mathematical Models and Finite Elements for Reservoir Simulation*. Elsevier, North-Holland, 1978.

[15] L. Chen. *i*FEM: an innovative finite element methods package in MATLAB. Technical report, University of California at Irvine, 2008.
[16] Z. Chen, G. Huan, and Y. Ma. *Computational Methods for Multiphase Flows in Porous Media*. Siam, 2006.
[17] Z.-X. Chen, G. Bodvarsson, and P. Witherspoon. Comment on "Exact integral solutions for two-phase flow" by David B. McWhorter and Daniel K. Sunada. *Water Resour. Res*, 28:1477–1478, 1992.
[18] T. A. Davis. *Direct methods for sparse linear systems*, volume 2 of *Fundamentals of Algorithms*. Society for Industrial and Applied Mathematics (SIAM), Philadelphia, PA, 2006.
[19] A. Di Pietro and A. Ern. *Mathematical Aspects of Discontinuous Galerkin Methods*, volume 69 of *Mathématiques & Applications*. Springer, 2011.
[20] D. A. Di Pietro, A. Ern, and J.-L. Guermond. Discontinuous Galerkin methods for anisotropic semidefinite diffusion with advection. *SIAM J. Numer. Anal.*, 46(2):805–831, 2008.
[21] G. Enchéry, R. Eymard, and A. Michel. Numerical approximation of a two-phase flow problem in a porous medium with discontinuous capillary forces. *SIAM J. Numer. Anal.*, 43(6):2402–2422, 2006.
[22] Y. Epshteyn and B. Rivière. Fully implicit discontinuous finite element methods for two-phase flow. *Applied Numerical Mathematics*, 57:383–401, 2007.
[23] A. Ern and J.-L. Guermond. *Theory and practice of finite elements*, volume 159 of *Applied Mathematical Sciences*. Springer-Verlag, New York, 2004.
[24] A. Ern, I. Mozolevski, and L. Schuh. Accurate velocity reconstruction for discontinuous Galerkin approximations of two-phase porous media flows. *C. R. Math. Acad. Sci. Paris*, 347(9-10):551–554, 2009.
[25] A. Ern, I. Mozolevski, and L. Schuh. Discontinuous Galerkin approximation of two-phase flows in heterogeneous porous media with discontinuous capillary pressures. *Comput. Methods Appl. Mech. Engrg.*, 199(23-24):1491–1501, 2010.
[26] A. Ern, S. Nicaise, and M. Vohralík. An accurate H(div) flux reconstruction for discontinuous Galerkin approximation of elliptic problems. *C.R.Acad.Sci.Paris, Ser.I*, 375:709–712, 2007.
[27] A. Ern, A. F. Stephansen, and P. Zunino. A discontinuous Galerkin method with weighted averages for advection-diffusion equations with locally small and anisotropic diffusivity. *IMA J. Numer. Anal.*, 29(2):235–256, 2009.
[28] B. G. Ersland, M. S. Espedal, and R. Nybø. Numerical methods for flow in a porous medium with internal boundaries. *Comput. Geosci.*, 2(3):217–240, 1998.
[29] O. J. Eslinger. *Discontinuous Galerkin Finite Element Methods applied to two-phase, air-water flow problems*. PhD thesis, University of Texas at Austin, 2005.
[30] R. Fucík, J. Mikyška, M. Beneš, and T. H. Illangasekare. An improved semianalytical solution for verification of numerical models of two-phase flow in porous media. *Vadose Zone Journal*, 6(3):93–104, 2007.
[31] R. Fucík, J. Mikyška, M. Beneš, and T. H. Illangasekare. Semianalytical solution for two-phase flow in porous media with a discontinuity. *Vadose Zone Journal*, 7(3):1001–1009, 2008.
[32] M. Gockenbach. *Understanding and implementing the finite element method*. SIAM, 2006.
[33] R. Helmig. *Multiphase flow and transport processes in the subsurface*. Springer, 1997.
[34] J. S. Hesthaven and T. Warburton. *Nodal discontinuous Galerkin methods*, volume 54 of *Texts in Applied Mathematics*. Springer, New York, 2008. Algorithms, analysis, and applications.
[35] H. Hoteit and A. Firoozabadi. Numerical modeling of two-phase flow in heterogeneous permeable media with different capillary pressures. *Advances in Water Recources*, 31:56–73, 2008.
[36] W. Klieber and B. Rivière. Adaptive simulations of two-phase flow by discontinuous Galerkin methods. *Comput. Methods Appl. Mech. Engrg.*, 196(1-3):404–419, 2006.
[37] M. Leverett. Capillary behavior in porous solids. *Trans. AIME*, 142:152–169, 1941.
[38] D. McWhorter and D. Sunada. Exact integral solutions for twophase flow. *Water Resources Research*, 26(3):399–413, 1990.
[39] D. McWhorter and D. Sunada. Replay. *Water Resources Research*, 28:1479, 1992.
[40] D. Nayagum, G. Schäfer, and R. Mosè. Modelling two-phase incompressible flow in porous media using

mixed hybrid and discontinuous finite elements. *Computational Geosciences*, 8:49–73, 2004.

[41] M. Ohlberger. Convergence of a mixed finite elements–finite volume method for the two phase flow in porous media. *East-West J. Numer. Math.*, 5(3):183–210, 1997.

[42] B. Rivière. *Discontinuous Galerkin methods for solving elliptic and parabolic equations: Theory and implementation*. Frontiers in Mathematics. SIAM, Philadelphia, 2008.

[43] C. J. van Duijn, J. Molenaar, and M. J. Neef. The effect of capillary forces on immiscible two-phase flow in heterogeneous porous media. *Transport in Porous Media*, 21:71–93, 1995.

[44] C. J. van Duijn and M. J. Neef. Similarity solution for capillary redistribution of two phases in a porous medium with a single discontinuity. *Advances in Water Resourses*, 21:451–461, 1998.

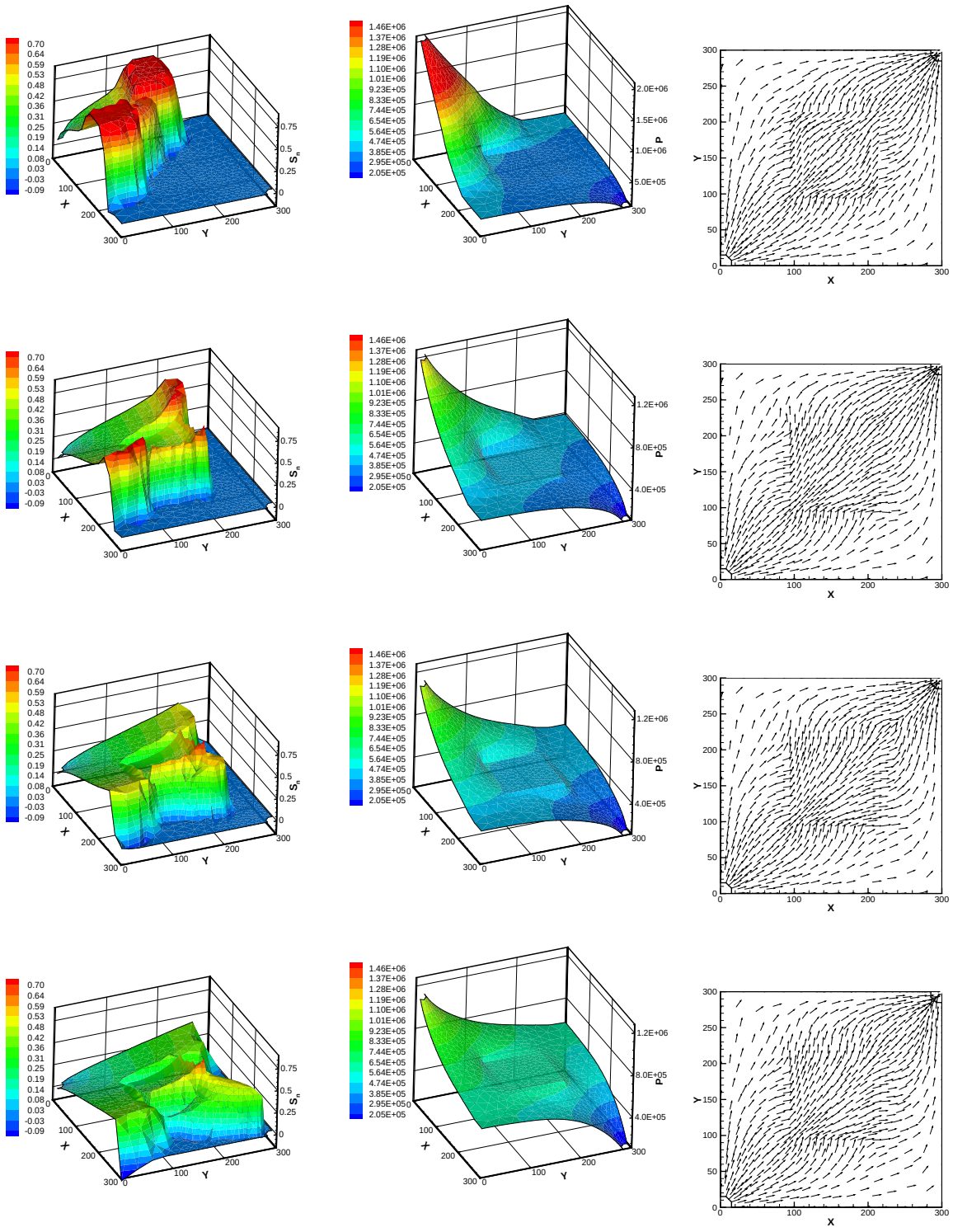

Figure 5: Saturation, global pressure and total velocity for test case 4a calculated on mesh $q(\mathcal{T}_h^{(a)})$. First line: $t = 70$ days, $\tau = 0.27$ days; second line: $t = 350$ days, $\tau = 0.62$ days; third line: $t = 725$ days, $\tau = 0.72$ days and fourth line: $t = 1800$ days, $\tau = 0.7$ days.

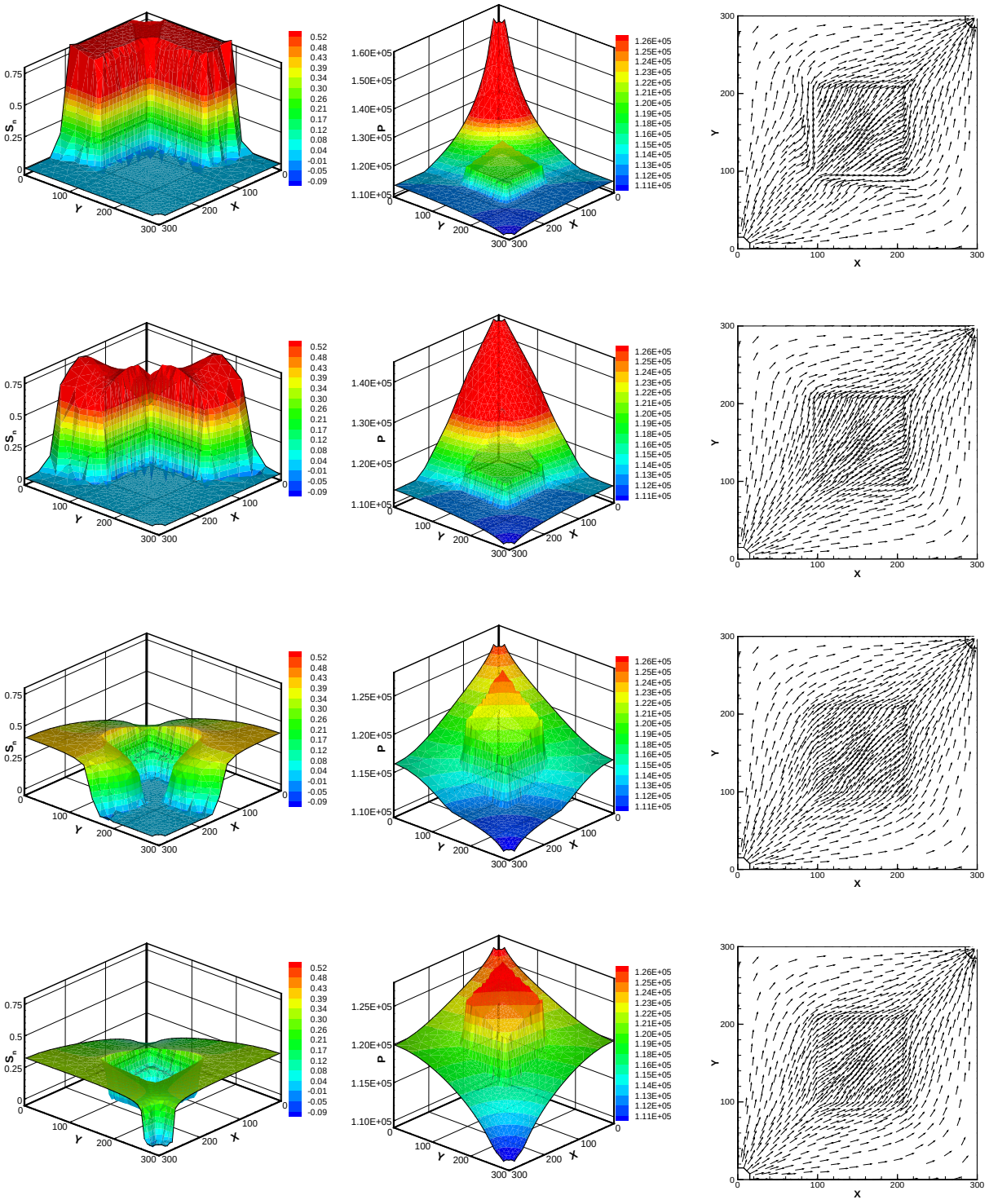

Figure 6: Saturation, global pressure and total velocity for test case 4b calculated on mesh $q(\mathcal{T}_h^{(b)})$. First line: $t = 2$ days, $\tau = 0.12$ days, second line: $t = 60$ days, $\tau = 0.74$ days; third line: $t = 950$ days, $\tau = 6$ days and fourth line: $t = 2970$ days, $\tau = 10$ days.